

# Dynamic vaccination in partially overlapped multiplex network

L. G. Alvarez-Zuzek\* and M. A. Di Muro

*Departamento de Física, Facultad de Ciencias Exactas y Naturales,  
Universidad Nacional de Mar del Plata,  
and Instituto de Investigaciones Físicas de Mar del Plata (IFIMAR-CONICET),  
Deán Funes 3350, 7600 Mar del Plata, Argentina.*

Shlomo Havlin

*Department of Physics, Bar-Ilan University, Ramat-Gan 52900, Israel.*

L. A. Braunstein

*Departamento de Física, Facultad de Ciencias Exactas y Naturales,  
Universidad Nacional de Mar del Plata,  
and Instituto de Investigaciones Físicas de Mar del Plata (IFIMAR-CONICET),  
Deán Funes 3350, 7600 Mar del Plata, Argentina. and  
Center for Polymer Studies, Boston University,  
Boston, Massachusetts 02215, USA.*

(Dated: January 16, 2019)

## Abstract

The spread of epidemics has always been a matter of interest due to its catastrophic effects that it may inflict in a society. This issue has been behind the motivation of many investigations that tried to develop and study different mitigation strategies to diminish the impact of diseases spreading in populations. Remarkable epidemic spreading cases, like the H1N1 pandemic (2009) and the Ebola outbreak in Africa (2014), and their catastrophic consequences worldwide, have motivated the scientific community to investigate extensively how to develop new efficient mitigation strategies to avoid catastrophic damages in future epidemics outbreaks. In this work we propose and investigate a new strategy of vaccination, which we call “dynamic vaccination”. In our model, susceptible people become aware that one or more of their contacts are infected, and thereby get vaccinated with probability  $\omega$ , before having physical contact with any infected patient. Then, the non-vaccinated individuals will be infected with probability  $\beta$ . We apply the strategy to the SIR epidemic model in a multiplex network composed by two networks, where a fraction  $q$  of the nodes acts in both networks. We map this model of dynamic vaccination into bond percolation model, and use the generating functions framework to predict theoretically the behavior of the relevant magnitudes of the system at the steady state. We find a perfect agreement between the solutions of the theoretical equations and the results of stochastic simulations. In addition, we find an interesting phase diagram in the plane  $\beta - \omega$ , which is composed by an epidemic and a non-epidemic phases, separated by a critical threshold line  $\beta_c$ , which depends on  $q$ . As  $q$  decreases,  $\beta_c$  increases, *i.e.*, as the overlap decreases, the system is more disconnected, therefore more virulent diseases are needed to spread epidemics. Surprisingly we find that, for all values of  $q$ , a region in the diagram where the vaccination is so efficient that, regardless of the virulence of the disease, it never becomes an epidemic. We compare our strategy with random immunization and find that vaccinating dynamically is much more efficient. Using the same amount of vaccines for both scenarios, we obtain that the spread of the disease is much lower in the case of dynamic vaccination.

---

\* lgalvere@mdp.edu.ar

## I. INTRODUCTION

In 2009, the pandemic virus (H1N1) was identified as the cause of many cases of human illnesses in California and Texas and a severe outbreak in Mexico. The pandemic had a reproduction value of approximately 1.5 and appeared to exhibit a community transmissibility similar to the respiratory pathogen SARS coronavirus (SARS-CoV). Even though the most commonly affected age group was 5-45 years old, the influenza also affected other age groups, such as older adults, pregnant women and children. By the end of the pandemic in 2010, it was registered that the virus caused the death of around twenty thousand people all over the world, and it was fueled by the mobility between regions and different countries. In [1] the authors studied the role of travel restrictions in halting pandemics, by using short-range mobility data, and explored alternative scenarios by assessing the potential impact of mobility restrictions. However, although this strategy could be very effective, it was found only useful to slow down the spread of the diseases, which might give time to the health authorities to develop a better strategy to stop the epidemic, for example the development of a new vaccine. Fortunately, in the case of the H1N1 pandemic, it was possible to develop and deploy a vaccination campaign, just in time to prevent a further spreading of the disease.

It is well known that infectious diseases usually spread by physical contact between individuals in a society [2, 3]. Over the years, researchers have found that the best way to model these types of contact patterns [4–6] is by using the topology of complex networks [7–11], where people are represented by nodes, and their interactions, as links. A commonly-used model for reproducing the dynamics of the spreading of endemic diseases, such as seasonal influenza or SARS [12], is the susceptible-infected-recovered (SIR) model [13–15]. This model groups individuals of a population into three compartments according to their state: susceptible (S), infected (I), and recovered (R). When a susceptible individual is in contact with an infected one, it becomes infected with probability  $\beta$ , which is the same for everyone. Infected individuals recover after a period of time  $t_r$ , *i.e.*, they become immunized and cannot be infected again or infect others. When the parameters  $\beta$  and  $t_r$  are constant, the effective probability of infection is given by the transmissibility  $T = 1 - (1 - \beta)^{t_r}$  [16, 17]. The SIR model has a tree-like structure with branches of infection that develop and expand, and this is because infected individuals cannot be re-

infected, so the infection can only move forwards. It has been proven that this process can be mapped into link percolation [18, 19], and thus the dynamic can be described using the generating function framework. The most important property in this framework is the probability  $f$  that a branch of infection will expand throughout the network [19]. When a branch of infection reaches a node with  $k$  connections across one of its links, it can only expand through its  $k - 1$  remaining connections. It can be shown that  $f$  verifies the self-consistent equation  $f = 1 - G_1(1 - Tf)$ , where  $G_1(x) = \sum_{k=k_{\min}}^{k_{\max}} kP(k)/\langle k \rangle x^{k-1}$  is the generating function of the underlying branching process [18]. Note that  $G_1(x)$  represents the probability that the branches of infection do not expand throughout the network. In the steady state of this process, there is a critical threshold  $T_c$  that separates an epidemic phase from a non-epidemic phase. When  $T \leq T_c$  there is an epidemic-free phase with only small outbreaks, which corresponds to finite clusters in link percolation theory. But, when  $T > T_c$  an epidemic phase develops, the branches of infection contribute to a spanning cluster of recovered, previously infected, individuals. Thus, the probability of selecting a random node that belongs to the spanning cluster is given by  $R = 1 - G_0(1 - Tf)$ , where  $G_0(x) = \sum_{k=k_{\min}}^{k_{\max}} P(k)x^k$  is the generating function of the degree distribution.

The spread of epidemics in networks [20–23] have been the focus of motivation of several investigations that seek to develop and study different strategies of mitigation for decreasing the impact of diseases on healthy populations [13, 24–28]. On one hand, referring to non-pharmaceutical strategies, one of the most common and studied is “quarantine”, in which all individuals of the affected population must remain in isolation for a period of time. This scenario is difficult to perform, besides it involves a great economic loss. On the other hand, a more moderate strategy proposed is “social distancing” [29, 30], in which those susceptible individuals distance themselves from those infected individuals or from those who present the symptoms of the disease. Although all these strategies are beneficial, but with no doubt the most effective one is “vaccination” [31] if available. In the early times *random vaccination* has been studied [32]. In this protocol susceptible individuals are vaccinated regardless of whether there are or not in contact with an infected individual. However, this strategy requires a huge amount of vaccines and resources that may not be available. One way to improve this strategy is *targeted vaccination* [33], that is to vaccinate those people that have many connections, and therefore, higher probability of getting the disease and transmitting it. However, this strategy is difficult to implement,

since the degrees of nodes in the network must be known in detail. In [34], the authors proposed the *acquaintance immunization* strategy which does not require knowledge of degrees. They choose a number of nodes at random and point for each one of his nearest neighbors. Then, those nearest neighbors are selected for immunization. So, given that a randomly chosen link points with high probability to a high degree node, this is actually a preferential immunization of the hubs, which reduces dramatically the amount of vaccines needed.

Since the advent of multilayer networks or network of networks [35–48], these structures have been the focus of much research and have allowed the scientific community to use a more realistic approach. With this new insight, the spread of epidemics was once again a thrive subject to investigate [27, 49–51]. On top of that, the cases of the H1N1 pandemic (2009) and the Ebola outbreak in Africa (2014), and their catastrophic consequences worldwide, have prompted the research of new mitigation strategies to avoid similar damages in future epidemics outbreaks [30, 52–58]. With this motivation in mind, we propose a new vaccination strategy to prevent a disease from becoming an epidemic. We call our strategy “dynamic vaccination” and we are interested in studying how epidemic spreads in the presence of this new protocol of vaccination. In our model, the group of susceptible people that have a relation with infected individuals, is the target of the immunization strategy. The contacts or neighbors of an infected person receives a vaccine with a probability  $\omega$ . If the susceptible individuals are vaccinated, they acquire immunization and cannot be infected or infect others anymore.

We develop our epidemic model taking into account this new vaccination rule, over an overlapped multiplex network substrate composed of two networks. We perform stochastic simulations and we apply the generating functions framework to develop theoretical equations that describe the outcome of the model. We find an excellent match between the simulation results and the solutions of the analytical set of equations.

The paper is organized as follows: in Section I we present a brief introduction to the topic. Section II explains the model and the results obtained. This section is divided in three parts *A*, *B* and *C*. In *A* we present the rules of the epidemic model with the dynamic vaccination. Then, in *B* we develop the theory that corresponds to the epidemic spreading problem. Lastly, in *C* we show the simulations results and compare them with the results of the theoretical equations, which are solved numerically. Finally, in Section

III we present our discussions and outlook.

## II. MODEL AND RESULTS

Our epidemic model is performed on a multiplex system composed of two networks  $A$  and  $B$ , each one characterized by a degree distribution  $P^\alpha(k)$ , with  $\alpha = A, B$ . Both networks are connected to each other through a fraction  $q$  identical pairs of nodes in both networks [51]. Those pairs of nodes in network  $A$  and  $B$  represent the same individual acting in different networks. For example one network could represent the personal contacts of the individuals at their workplace, and the other network their family or friends.

### A. Model

At the initial stage of the Susceptible-Infected-Vaccinated-Recovered model (SI-R/V) all individuals in both networks are susceptible. We randomly infect an individual in network  $A$ , which we call patient zero, and also its counterpart in network  $B$ , in case it belongs to both networks. Then, all the neighbors of this patient zero (in both networks,  $A$  and  $B$ ) will be vaccinated and hence immunized with probability  $\omega$ . For the sake of simplicity, we consider that this probability is the same for all individuals. On the other hand, those neighbors who did not get vaccinated will be infected with probability  $(1 - \omega)\beta$ . Once an individual receive a vaccine, it can no longer acquire the disease and becomes immunized. Infected individuals will recover after  $t_r$  time steps and can not be affected by the disease anymore. In Fig. 1 we demonstrate the dynamic of our model for  $t_r = 1, 2, 3$  and  $4$  and  $q = 0.7$ .

We demonstrate the model in Fig. 1. At the beginning of the dynamic, at  $t = 1$ , there is only one infected node (patient zero - in red). In network  $A$ , this individual has two neighbors: one of them gets vaccinated with probability  $\omega$ , and the other one becomes infected with probability  $(1 - \omega)\beta$ . As both individuals are present in both networks, their counterparts in network  $B$  are also vaccinated and infected, respectively. At  $t = 2$ , patient zero recovers in both networks and the new infected individuals will try to infect their susceptible neighbors. In network  $A$ , one of the new infected individuals has only one vaccinated neighbor, thus he cannot spread the disease, and the other has

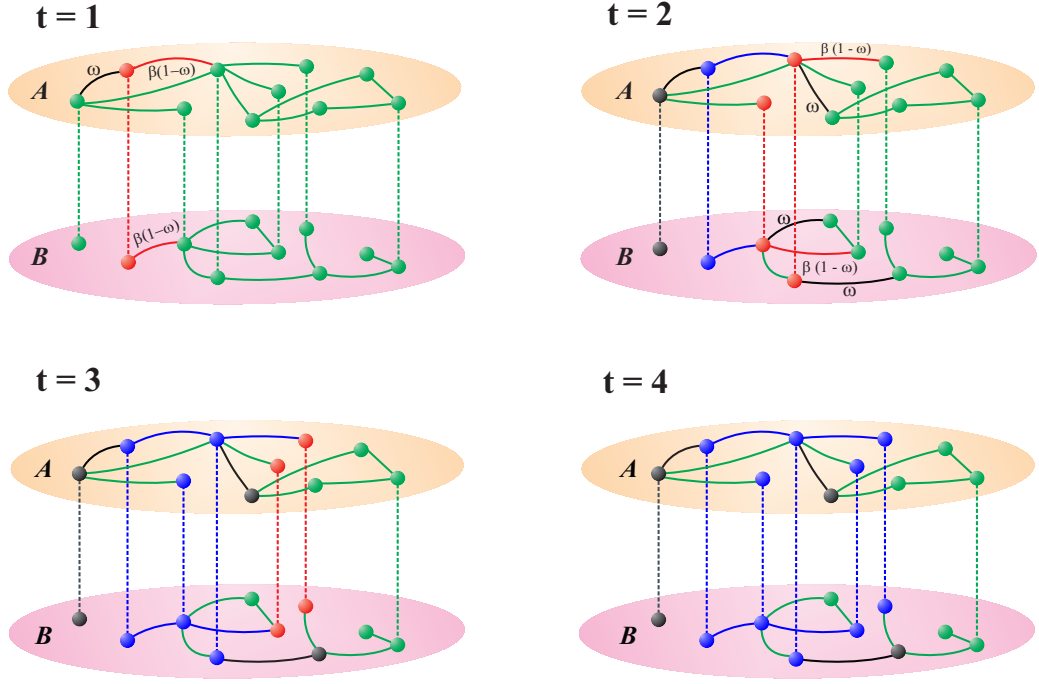


FIG. 1. **Schematic of the SI-R/V epidemic process** in a multiplex network consisting of two networks, each of size  $N = 10$ . A fraction  $q$  of nodes in both networks represent the same individual acting in different environments, Here  $q = 0.7$ . The colors of the nodes represent the following states: green (●) for Susceptible (S), red (●) for Infected (I), blue (●) for recovered (R) and violet (●) for vaccinated individuals. In this case, we assume  $t_r = 1$ . At  $t = 1$ , the patient zero infects one of its neighbors in network  $A$  and the other becomes vaccinated. Since this infected patient is present in both networks, it can also spread the disease in network  $B$ . The red lines indicate the direction of the branches of infection. In the next time step,  $t = 2$ , this patient zero recover in both networks and the new infected individuals continue spreading the disease. The process continues until the fourth temporary step, which is the steady state, where there are no more infected individuals that can continue spreading the disease.

three susceptible neighbors: one gets vaccinated, the other becomes infected, as well as his counterpart in network  $B$ , while the last remains susceptible. In network  $B$  there are two infected individuals, of which only one manages to infect one of its neighbors. At the next time step, this infected individual recovers and the newly infected individuals continue to spread the disease. The dynamic continues until the system reaches a steady state in which there are no more infected nodes ( $t = 4$ ) and the epidemic ends.

## B. Theory

In our model of the SI-R/V process we assume that the transmissibility is the same in both networks because the disease that spreads in one networks is the same as in the other network, and all individuals in the system spread the infection equally. As we mentioned earlier, each infected individual in each network can infect each one of its neighbors (with probability  $\beta$ ), if they have not been vaccinated earlier (with probability  $(1-\omega)$ ). Thus, at each time step the probability that an infected node infects a susceptible neighbor is  $(1-\omega)\beta$  during a period of time  $t_r$ , after which he recovers. Then, the overall transmissibility  $T_\beta \equiv T(\beta, t_r, w)$  is the probability that an infected individual will transmit the disease to its neighbors, which is given by,

$$T_\beta = (1-\omega)\beta \sum_{t=1}^{t_r} [(1-\omega)(1-\beta)]^{t-1} = \frac{1 - (1-\omega)^{t_r}(1-\beta)^{t_r}}{\omega + \beta - \omega\beta} (1-\omega)\beta. \quad (1)$$

Using the generating function framework and mapping this process onto link percolation in two networks [18, 19], we can write two self-consistent coupled equations,  $f_{A/B}$ , for the probability that following a random chosen edge a branch of infection will spread the infection,

$$\begin{aligned} f_A &= (1-q) [1 - G_1^A(1 - T_\beta f_A)] + q [1 - G_1^A(1 - T_\beta f_A) G_0^B(1 - T_\beta f_B)], \\ f_B &= (1-q) [1 - G_1^B(1 - T_\beta f_B)] + q [1 - G_1^B(1 - T_\beta f_B) G_0^A(1 - T_\beta f_A)]. \end{aligned} \quad (2)$$

Here,  $G_0^{A/B}(x)$  and  $G_1^{A/B}(x)$  are the generating functions of the degree and the excess degree distributions for each network respectively. On one hand,  $G_1^{A/B}(x)$  represents the probability that choosing a random edge that leads to a node of degree  $k$  in one network, this branch cannot spread the disease through its remaining  $k-1$  connections. On the other hand,  $G_0^{A/B}(x)$  takes into account the probability that, if the counterpart node of degree  $k$  in the other network  $B/A$  is present, the branch does not spread from one network to the other through its  $k$  links in  $B/A$ .

In Eqs. (2) the first term in both equations corresponds to those branches of infection that only spread within their own network, while the second term takes into account those branches that spread through both networks.



During the dynamics, the branches of infection reaches both recovered and vaccinated nodes. The difference is that once the infection branch crosses a link to reach a node that has been vaccinated, this vaccinated individual cannot spread the disease. Thus, we can develop in the same way as before, a transmissibility  $T_\omega \equiv T(\beta, t_r, \omega)$  as the effective probability that a susceptible neighbor in contact with an infected node, for a period of time  $t_r$ , will be vaccinated. This transmissibility is given by,

$$T_\omega = \omega \sum_{t=1}^{t_r} [(1-\omega)(1-\beta)]^{t-1} = \frac{1 - (1-\omega)^{t_r}(1-\beta)^{t_r}}{\omega + \beta - \omega\beta} \omega. \quad (3)$$

Therefore, in the steady state of our model, the magnitude that maps with the order parameter of link percolation is not only the fraction of recovered individuals, as in the common SIR [13], but instead, it is the sum of vaccinated and recovered, i.e.,  $V + R$ . This is due to the fact that the infection branches also reaches those nodes that were vaccinated via crossing a link. To consider this analytically, a multiplicative term must be added. This term takes into account the weights of the probability of infection (or vaccination) among all the events that may occur to cross the link  $I \rightarrow S$ . Then the fraction of recovered individuals in each network can be written as

$$\begin{aligned} R_A &= \frac{T_\beta}{T_\beta + T_\omega} \{ (1-q) [1 - G_0^A(1 - T_\beta f_A)] + q [1 - G_0^A(1 - T_\beta f_A) G_0^B(1 - T_\beta f_B)] \}, \\ R_B &= \frac{T_\beta}{T_\beta + T_\omega} \{ (1-q) [1 - G_0^B(1 - T_\beta f_B)] + q [1 - G_0^B(1 - T_\beta f_B) G_0^A(1 - T_\beta f_A)] \}. \end{aligned} \quad (4)$$

And the fraction of vaccinated nodes is given by,

$$\begin{aligned} V_A &= \frac{T_\omega}{T_\omega + T_\beta} \{ (1-q) [1 - G_0^A(1 - T_\beta f_A)] + q [1 - G_0^A(1 - T_\beta f_A) G_0^B(1 - T_\beta f_B)] \}, \\ V_B &= \frac{T_\omega}{T_\omega + T_\beta} \{ (1-q) [1 - G_0^B(1 - T_\beta f_B)] + q [1 - G_0^B(1 - T_\beta f_B) G_0^A(1 - T_\beta f_A)] \}. \end{aligned} \quad (5)$$

Then, the total fraction of recovered (R) and vaccinated (V) individuals in the system is given by,

$$\begin{aligned} R &= (R_A + R_B - \zeta_R)/(2 - q) \\ V &= (V_A + V_B - \zeta_V)/(2 - q), \end{aligned} \quad (6)$$

where  $\zeta_R = \frac{T_\beta}{T_\omega + T_\beta} q [1 - G_0^A(1 - T_\beta f_A) G_0^B(1 - T_\beta f_B)]$  is the fraction of shared nodes that are recovered and  $\zeta_V = \frac{T_\omega}{T_\omega + T_\beta} q [1 - G_0^A(1 - T_\beta f_A) G_0^B(1 - T_\beta f_B)]$  is the fraction of shared nodes that are vaccinated, in the steady state.

From Eqs. (1) and (2) we can see that if we use the total transmissibility, which is the sum of  $T_\beta$  and  $T_\omega$ , as the control parameter we lose information about the probability of vaccination,  $\omega$  (see Appendix IV A). Hence, we will make use of the virulence of the diseases  $\beta = \beta_T$  as the control parameter. To this end, we fixed  $t_r = 1$  and obtain  $\beta$  by inverting Eq. (1).

### C. Simulation Results

In the simulations, we generate two uncorrelated networks,  $A$  and  $B$ , of equal size  $N = 10^5$  using the Molloy-Reed algorithm [59]. We randomly overlap a fraction  $q$  of nodes in network  $A$  with nodes in network  $B$  by a one-to-one connection, where one network represents for example an individual's work relations and the other their social relations. The degree distribution in each network is given by  $P_i(k)$ , with  $i = A, B$  and  $k_{\min} \leq k \leq k_{\max}$ , where  $k_{\min}$  and  $k_{\max}$  are the minimum and the maximum degree that a node can have. We assume that an epidemic occurs in a realization if the number of recovered individuals is greater than 200 [60, 61]. To calculate the total number of recovered and vaccinated nodes throughout the entire system, the pair of nodes that act in both networks are counted as single nodes, as they represent the same individual. In Fig. 2 we show the total number of recovered (R) and vaccinated (V) nodes as a function of  $\beta$  for several values of  $\omega$ . For two coupled Erdős-Rényi (ER) networks [62], with average degree  $\langle k_A \rangle = \langle k_B \rangle = 5$  and  $k_{\min} = 0$  and  $k_{\max} = 40$ . Each curve corresponds to a different value of  $\omega$ , for  $\omega \in [0.1, 0.8]$  with  $\Delta\omega = 0.1$  from left to right. For the sake of simplicity we set  $t_r = 1$  and consider the cases of  $q = 0.3$  ((a) and (b)), and  $q = 0.7$  ((c) and (d)). Insets in Fig. 2 (a) and 2 (c) correspond to the critical threshold as a function of  $\omega$ . While, in Fig. 2 (b) and 2(d) the insets correspond to the maximum in the fraction of vaccinated individuals  $V_{peak}$ , if there is one, as a function of  $\omega$ .

Figure 2 shows excellent agreement between simulation results and the theoretical analysis (Eqs. (4) and (6)). As can be seen, the critical threshold  $\beta_c$  increases as  $q$  decreases. Hence, for less interconnected networks a more virulent disease is needed in order to become an epidemic. For instance, for the case of  $\omega = 0.8$  there is a noticeable difference in  $\beta_c$  for the different  $q$ . However, it can be seen that qualitatively, the behavior of the curves, for R and V, are very similar regardless the overlap.

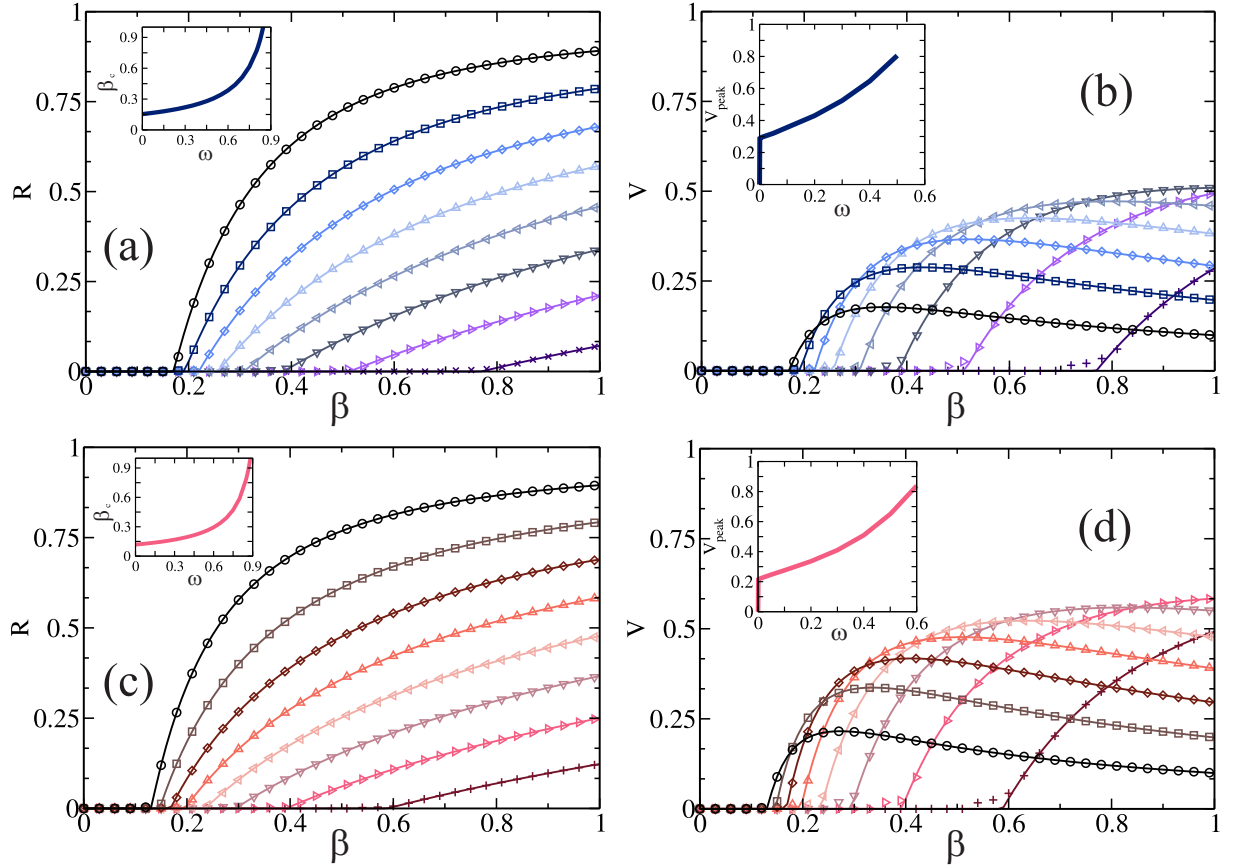


FIG. 2. **Theoretical and Simulation results** of the total fraction of recovered ( $R$ ) and vaccinated ( $V$ ) nodes as a function of the virulence of the diseases  $\beta$  and for different values of  $\omega$ , in the steady state of the process. We consider  $t_r = 1$ , (a)-(b)  $q = 0.3$  and (c)-(d)  $q = 0.7$ , and different values of  $\omega \in [0.1, 0.8]$  with  $\Delta\omega = 0.1$  from left to right. The symbols correspond to the simulation results and the lines correspond to the theoretical evaluation of Eqs. (6). Insets in (a) and (c) corresponds to the critical threshold value  $\beta_c$  as a function of  $\omega$ . Insets in (b) and (d) corresponds to the maximum value of  $V$ , as a function of  $\omega$ . The multiplex network consist of two ER networks, each of size  $N = 10^5$  and  $\langle k_A \rangle = \langle k_B \rangle = 5$  with  $k_{min} = 0$  and  $k_{max} = 40$ . Simulation results are averaged over  $10^4$  realizations.

In Fig. 2(a) and 2(c) we can see that as  $\omega$  increases the total fraction of recovered nodes decreases. For high values of  $\beta$ , such as  $\beta = 1$ , when  $\omega = 0.1$  the disease reaches 90% of the population, but for the case of  $\omega = 0.8$  it reaches only less than 10%. Besides, as  $\omega$  increases the critical threshold  $\beta_c$  also increases, *i.e.*, as we vaccinate with higher probability a more virulent disease will be needed to reach the entire system. This behavior

can be seen in the inset of the figures, where we plot  $\beta_c$  as a function of  $\omega$ . Notice that for  $\omega \gtrsim 0.8$  the disease never becomes an epidemic.

In contrast, in Fig. 2(b) and 2(d), we can see that the total fraction of vaccinated nodes does not behave monotonically with  $\beta$ . For small beta  $V$  increases until it reaches a maximum value, then starts to decrease. This maximum value varies with  $\omega$ , is more pronounced for low values of  $\omega$  and vanishes as  $\omega$  becomes larger. The inset in each plot shows this peak as a function of  $\omega$ . When the probability of vaccination is equal to zero, there is no vaccinated nodes. However, slightly above  $\omega = 0$  a peak exhibits. Then, as  $\omega$  increases the fraction of vaccinated individuals in the peak also increases reaching a certain value of  $\omega$  above which the peak vanishes. Note that this maximum value also varies with the overlap fraction,  $q$ .

The origin of the peaks is the competition between the spread of the disease and the vaccination process. For instance, let's consider the case of low values of  $\omega$ , such as  $\omega = 0.1$  (black line). Slightly above  $\beta_c$ , the disease is not virulent enough so, increasing  $\beta$  the number infected and vaccinated increases. This is true until a certain value of  $\beta$ , that corresponds to the peak in  $V$ , above which individuals are more likely to become infected rather than vaccinated.

On the contrary, in the case of high  $\omega$  values, the peak is not exhibited. This is due to the fact that the virulence of the disease is not strong enough to overcome the vaccination. Furthermore, as  $\omega$  increases and for higher values of overlap the fraction of vaccinated individuals is much higher than for weakly connected networks. Note the limiting case of  $\beta = 1$  and  $\omega = 0.8$ , for  $q = 0.3$  (see Fig. 2(b)),  $V$  is almost a fraction of 0.3 of the population while for  $q = 0.7$  (see Fig. 2(d)) it reaches almost 0.5.

Focusing on the critical threshold  $\beta_c$ , this can be obtained theoretically from the intersection of the two Eqs. (2) where all branches of infection stop spreading, which is given when  $f_A = f_B = 0$ . This is equivalent to find the solution of the system  $\det(J - I) = 0$  where  $I$  is the identity matrix and  $J$  is the Jacobian matrix of the coupled equation with  $J_{i,k}|_{f_i=f_k=0} = \partial f_i / \partial f_k|_{f_i=f_k=0}$ . In [51, 57] this theoretical result has been obtained for the case of the common SIR model [13]. The difference in our model lies in the transmissibility and its dependence on  $\omega$ . Thus, we will present the critical threshold for  $\beta$ , its

dependence on  $\omega$ , and for simplicity we consider the case  $t_r = 1$ ,

$$\beta_c = \frac{[(\kappa_A - 1) + (\kappa_B - 1)] - \sqrt{[(\kappa_A - 1) - (\kappa_B - 1)]^2 + \frac{4q^2 \langle k_A \rangle \langle k_B \rangle}{(1-\omega)}}}{2(\kappa_A - 1)(\kappa_B - 1) - 2q^2 \langle k_A \rangle \langle k_B \rangle}, \quad (7)$$

where  $\langle k_A \rangle$  and  $\langle k_B \rangle$  are the average degree and  $\kappa_A = \frac{\langle k_A^2 \rangle}{\langle k_A \rangle}$  and  $\kappa_B = \frac{\langle k_B^2 \rangle}{\langle k_B \rangle}$  are the branching factor of networks  $A$  and  $B$ . Using numerical evaluations for the roots of the equation we find a physical and stable solution for  $\beta_c$ , which corresponds to the smaller root [63].

In Fig. 3 the phase diagram in the plane  $\beta - \omega$  is shown. We consider the cases of (a) two ER multiplex networks with average degree  $\langle k_A \rangle \simeq \langle k_B \rangle = 5$  and (b) two scale free networks where  $P_i(k_i) \sim k_i^{-\lambda_i} e^{-k_i/c}$  with  $\lambda_A = \lambda_B = 2.5$ ,  $k_{min} = 2$ ,  $k_{max} = \sqrt{N}$  and an exponential cutoff  $c = 50$  [18]. Note that this type of SF networks are appropriate to describe scenarios and structures of real-world systems [64]. We set  $t_r = 1$  and we vary the overlap between networks  $q \in [0, 1]$  with  $\Delta q = 0.1$ , from top to bottom.

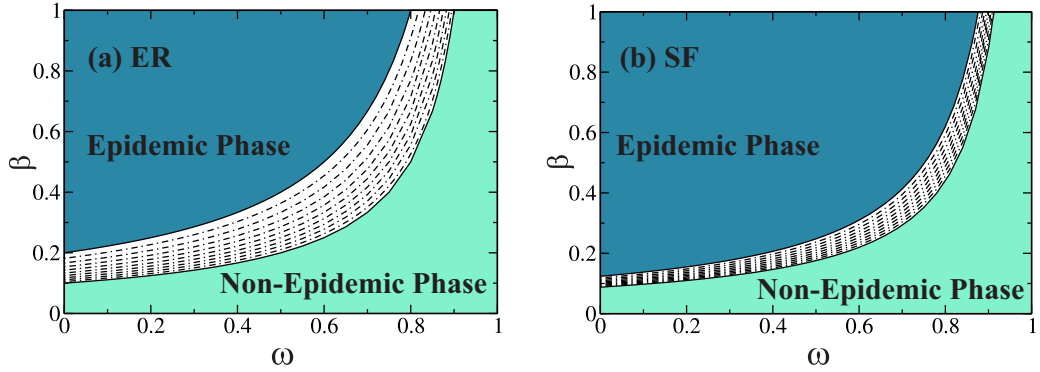


FIG. 3. **Phase diagram in the plane  $\beta - \omega$ .** All lines correspond to  $\beta_c$  obtained theoretically for  $t_r = 1$  and different values of  $q \in [0, 1]$  with  $\Delta q = 0.1$  from top to bottom. We consider in (a) two ER networks with  $\langle k_A \rangle = \langle k_B \rangle = 5$  with  $k_{min} = 0$  and  $k_{max} = 40$ , and in (b) two scale free networks, where  $P(k)^\alpha \propto k^{-\lambda_\alpha} e^{-k/c}$ ,  $\alpha = A, B$ , with  $\lambda_A = \lambda_B = 2.5$ ,  $k_{min} = 2$ ,  $k_{max} = \sqrt{N}$  and exponential cutoff  $c = 50$ . The region above each line corresponds to the epidemic phase and the region below corresponds to the non-epidemic phase. As we increase  $q$  both networks are more connected to each other which facilitates the spread of the epidemic, thus  $\beta_c$  decreases and the epidemic phase regime is reduced. In both figures there is a critical value of  $\omega$  above which regardless of the virulence of the disease, it never becomes an epidemic. In the limit of  $\omega = 0$  we recover the regular SIR in multiplex networks and as  $\omega$  increases, there will be more vaccinated individuals so  $\beta_c$  increases.

From Figure (3) we can see two phases: one epidemic and the other epidemic-free. The different curves, which correspond to different values of the overlap  $q$ , separate the epidemic phase from the epidemic-free phase. We can see that as  $q$  decreases and  $\omega$  increases the non-epidemic phase increases. As we increase  $\omega$ , for all values of  $q$ , we can see the existence of a threshold above which, even for very virulent diseases, the outbreak will never become epidemic. The behavior of Fig. 3(a) and Fig. 3(b) is similar. However, it can be seen a smaller difference in  $\beta_c$  as we vary the overlap in SF networks.

Finally, in Fig. 4 we compare our vaccination strategy results with random immunization, on top of a multiplex network structure [58]. We consider the case of (a)-(b) two ER multiplex networks with the same average degree equal to  $\langle k_{A/B} \rangle = 5$  and (c)-(d) two scale free networks where with  $\lambda_A = \lambda_B = 2.5$ . We set  $t_r = 1$ ,  $\beta = 0.3$  and vary the overlap between networks (a)-(c)  $q = 0.3$  and (c)-(d)  $q = 0.7$ . Fig. 4 shows the total fraction of recovered nodes in the steady state as a function of  $V$  and  $\omega$ . For example, in (a) when the total fraction of vaccinated individuals is  $V = 0.2$ , for the case of random vaccination  $R \simeq 0.6$ . While, for our strategy dynamic vaccination there are two possible outcomes depending on  $\omega$ . If  $\omega \simeq 0.3$  then  $R \simeq 0.4$  but for the case of  $\omega \simeq 0.6$  we have a much more interesting scenario where the final fraction of recovered is close to zero ( $R \simeq 0.1$ ).

From Fig.4 we can see that, for same amount of vaccinated individuals, the number of recovered individuals is significantly lower for the case of dynamic vaccination. This behavior is seen in all plots, which indicates that our strategy is significantly more effective than random vaccination. Especially, in more heterogeneous networks, such as SF networks, we can see that this strategy is even more efficient.

On the other hand, when the system is more interconnected, the disease spreads more. Therefore, more vaccines are needed to prevented it from becoming an epidemic. For example, for a final fraction of recovered individuals equal to 20% of the population, it is required to vaccinate a fraction of individuals equal to  $V(q = 0.3) \simeq 0.25$  and  $V(q = 0.7) \simeq 0.4$ .

To summarize, we demonstrate that, on top of a multiplex network structure, dynamic vaccination strategy is much more efficient than random immunization. Using the same amount of vaccines, the total fraction of recovered individuals is always lower in the case of dynamic vaccination. Besides, in our strategy, depending on the parameters, we obtain

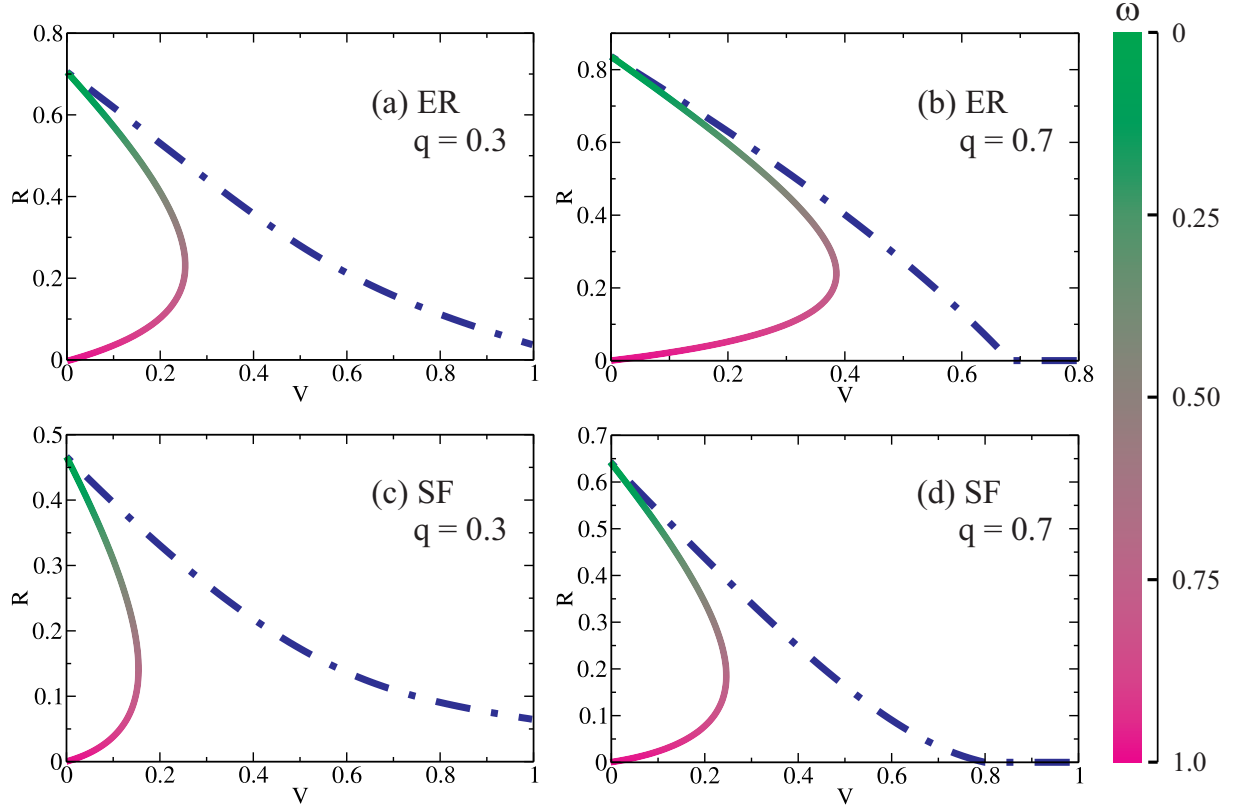


FIG. 4. **Comparison between dynamic and random vaccination.** Theoretical results of the total fraction of recovered ( $R$ ) nodes as a function of  $V$  and  $\omega$ . All dashed lines correspond to random vaccination and colored lines correspond to our strategy of dynamic vaccination for  $t_r = 1$  and  $\beta = 0.3$  and different values of overlap (a)-(c)  $q = 0.3$  and (b)-(d)  $q = 0.7$ . We consider in (a)-(b) two ER networks with  $\langle k_A \rangle = \langle k_B \rangle = 5$  with  $k_{min} = 0$  and  $k_{max} = 40$ , and in (c)-(d) two scale free networks, where  $P(k)^\alpha \propto k^{-\lambda_\alpha} e^{-k/c}$ ,  $\alpha = A, B$ , with  $\lambda_A = \lambda_B = 2.5$ ,  $k_{min} = 2$ ,  $k_{max} = \sqrt{N}$  and exponential cutoff  $c = 50$ . In all plots the total fraction of recovered nodes is lower in the case of dynamic vaccination.

a region where regardless of the virulence of the disease it will never become an epidemic. In comparison, if we vaccinate the same number of individuals, the fraction recovered in dynamic immunization will always be below that obtained if we vaccinate at random. Due to this result, our strategy can be very beneficial to be implemented in real scenarios, for example in outbreaks of Ebola or influenza, such as H1N1.

### III. DISCUSSION

In summary, we studied a novel model of dynamic vaccination on a system of the topology of two partially overlapped multiplex network, where  $q$  is the fraction of overlapped nodes between them. In our model, susceptible individuals in contact with infected patients have the opportunity to be vaccinated before the their neighbors attempt to infect them. That is, each time an infected person comes in contact with a susceptible individual, this one will try to get vaccinated with probability  $\omega$  and if he does not succeed he will be infected with probability  $\beta$ . Each infected node is assumed to recover after  $t_r$  time steps and will become immunized. Besides, vaccinated nodes are also immunized and can not be infected or infect others. Mapping this process into bond percolation and using the framework of generating functions, we analyzed analytically the total fraction of recovered and vaccinated nodes in the steady state as a function of the virulence of the diseases  $\beta$  for different values of the  $\omega$  and  $q$ , and we found a perfect agreement between the theoretical and the simulation results. As expected we find that as  $\omega$  increases the epidemic threshold  $\beta_c$  becomes larger, and disappearing for very large values of  $\omega$ . We also find a peak, for certain values of the parameters, in the fraction of vaccinated nodes as a function of  $\omega$ , which is determined by the competition between the vaccination strategy and the spread of the disease. We find an interesting phase diagram in the plane  $\beta - \omega$ , where we can see an epidemic phase, which diminish as  $q$  and  $\omega$  increase, and a non-epidemic phase, where the diseases can not spread. A remarkable result of the phase diagram is that for certain values of  $q$  and  $\omega$ , regardless of the virulence of the disease, it will never become an epidemic. Finally, we demonstrate that our strategy is much more efficient than random immunization. In our model, vaccines are used in a more effective manner and therefore the total fraction of recovered individuals is lower.

### IV. ACKNOWLEDGMENTS

SH thanks the Israel Science Foundation, ONR, the Israel Ministry of Science and Technology (MOST) with the Italy Ministry of Foreign Affairs, BSF-NSF, MOST with the Japan Science and Technology Agency, the BIU Center for Research in Applied Cryptography and Cyber Security, and DTRA (Grant no. HDTRA-1-10-1- 0014) for financial



support. LGAZ, MAD and LAB wish to thank to UNMdP, FONCyT and CONICET (Pict 0429/2013, Pict 1407/2014 and PIP 00443/2014) for financial support.

- 
- [1] P. Bajardi, C. Poletto, J. J. Ramasco, M. Tizzoni, V. Colizza, and A. Vespignani, PLOS ONE **6**, 1 (2011).
  - [2] R. M. Anderson and R. M. May, *Infectious Diseases of Humans: Dynamics and Control* (Oxford University Press, Oxford, 1992).
  - [3] N. T. J. Bailey, *The Mathematical Theory of Infectious Diseases* (Griffin, London, 1975).
  - [4] C. Cattuto, W. V. den Broeck, A. Barrat, V. Colizza, J.-F. Pinton, and A. Vespignani, PLoS ONE **5**, e11596 (2010).
  - [5] M. C. Gonzalez, C. A. Hidalgo, and A.-L. Barabasi, Nature **453**, 779 (2008).
  - [6] J. Gómez-Gardeñes, V. Latora, Y. Moreno, and E. Profumo, Proceedings of the National Academy of Sciences **105**, 1399 (2008).
  - [7] S. Boccaletti, V. Latora, Y. Moreno, M. Chavez, and D. Hwang, Physics Reports **424**, 175 (2006).
  - [8] R. Cohen and S. Havlin, *Complex Networks: Structure, Robustness and Function* (Cambridge University Press, 2010).
  - [9] A. Barrat, M. Barthélemy, R. Pastor-Satorras, and A. Vespignani, Proc. Natl. Acad. Sci. USA **101**, 3747 (2004).
  - [10] M. E. J. Newman, *Networks: An Introduction* (Oxford University Press, 2010).
  - [11] R. Pastor-Satorras and A. Vespignani, Phys Rev Lett **86**, 3200 (2001).
  - [12] V. Colizza, A. Barrat, M. Barthélemy, and A. Vespignani, BMC Medicine **5**, 34 (2007).
  - [13] M. E. J. Newman, Physical Review E **66**, 016128 (2002).
  - [14] Y. Moreno, R. Pastor-Satorras, and A. Vespignani, The European Physical Journal B-Condensed Matter and Complex Systems **26**, 521 (2002).
  - [15] L. D. Valdez, P. A. Macri, and L. A. Braunstein, PLOS ONE **7**, 1 (2012).
  - [16] D. S. Callaway, M. E. J. Newman, S. H. Strogatz, and D. J. Watts, Physical Review Letters **85**, 5468 (2000).
  - [17] S. H. D. B.-A. R. Cohen, “Handbook of graphs and networks,” (Wiley-VCH, Berlin, 2002) Chap. Structural properties of scale free networks.

- [18] M. E. J. Newman, S. H. Strogatz, and D. J. Watts, *Physical Review E* **64**, 026118 (2001).
- [19] L. A. Braunstein, Z. Wu, Y. Chen, S. V. Buldyrev, T. Kalisky, S. Sreenivasan, R. Cohen, E. López, S. Havlin, and H. E. Stanley, *I. J. Bifurcation and Chaos* **17**, 2215 (2007).
- [20] C. Castellano and R. Pastor-Satorras, *Physical review letters* **105**, 218701 (2010).
- [21] R. Pastor-Satorras, C. Castellano, P. Van Mieghem, and A. Vespignani, *Rev. Mod. Phys.* **87**, 925 (2015).
- [22] M. De Domenico, C. Granell, M. A. Porter, and A. Arenas, *Nature Physics* (2016).
- [23] W. Wang, M. Tang, H. E. Stanley, and L. A. Braunstein, *Reports on Progress in Physics* **80**, 036603 (2017).
- [24] C. Buono, F. Vazquez, P. A. Macri, and L. A. Braunstein, *Phys. Rev. E* **88**, 022813 (2013).
- [25] C. Granell, S. Gómez, and A. Arenas, *Phys. Rev. Lett.* **111**, 128701 (2013).
- [26] E. Cozzo, R. A. Baños, S. Meloni, and Y. Moreno, *Phys. Rev. E* **88**, 050801(R) (2013).
- [27] J. Sanz, C.-Y. Xia, S. Meloni, and Y. Moreno, *Physical Review X* **4**, 041005 (2014).
- [28] C. Lagorio, M. Dickison, F. Vazquez, L. A. Braunstein, P. A. Macri, M. V. Migueles, S. Havlin, and H. E. Stanley, *Phys. Rev. E* **83**, 026102 (2011).
- [29] L. Valdez, P. Macri, and L. Braunstein, *Physica A: Statistical Mechanics and its Applications* **392**, 4172 (2012).
- [30] L. Wang, Y. Zhang, T. Huang, and X. Li, *Physical Review E* **86**, 032901 (2012).
- [31] Z. Wang, C. T. Bauch, S. Bhattacharyya, A. d’Onofrio, P. Manfredi, M. Perc, N. Perra, M. Salathé, and D. Zhao, *Physics Reports* **664**, 1 (2016).
- [32] R. Pastor-Satorras and A. Vespignani, *Phys. Rev. E* **65**, 036104 (2002).
- [33] N. Madar, T. Kalisky, R. Cohen, D. Ben-avraham, and S. Havlin, *The European physical journal b-condensed matter and complex systems* **38**, 269 (2004).
- [34] R. Cohen, S. Havlin, and D. ben Avraham, *Phys. Rev. Lett.* **91**, 247901 (2003).
- [35] S. V. Buldyrev, R. Parshani, G. Paul, H. E. Stanley, and S. Havlin, *Nature* **464**, 1025 (2010).
- [36] J. Gao, S. V. Buldyrev, S. Havlin, and H. E. Stanley, *Physical Review Letters* **107**, 195701 (2011).
- [37] J. Gao, S. V. Buldyrev, H. E. Stanley, and S. Havlin, *Nature Physics* **8**, 40 (2012).
- [38] G. Dong, J. Gao, R. Du, L. Tian, H. E. Stanley, and S. Havlin, *Physical Review E* **87**, 052804 (2013).

- [39] L. D. Valdez, P. A. Macri, H. E. Stanley, and L. A. Braunstein, *Physical Review E* **88**, 050803(R) (2013).
- [40] G. J. Baxter, S. N. Dorogovtsev, A. V. Goltsev, and J. F. F. Mendes, *Physical Review Letters* **109**, 248701 (2012).
- [41] C. D. Brummitt, R. M. D’Souza, and E. A. Leicht, *Proceedings of the National Academy of Sciences* **109**, 680 (2012).
- [42] C. D. Brummitt, K.-M. Lee, and K.-I. Goh, *Physical Review E* **85**, 045102(R) (2012).
- [43] K.-M. Lee, J. Y. Kim, W. K. Cho, K.-I. Goh, and I.-M. Kim, *New Journal of Physics* **14**, 033027 (2012).
- [44] S. Gómez, A. Díaz-Guilera, J. Gómez-Gardeñes, C. J. Pérez-Vicente, Y. Moreno, and A. Arenas, *Phys. Rev. Lett.* **110**, 028701 (2013).
- [45] J. Y. Kim and K.-I. Goh, *Physical Review Letters* **111**, 058702 (2013).
- [46] E. Cozzo, A. Arenas, and Y. Moreno, *Physical Review E* **86**, 036115 (2012).
- [47] A. Cardillo, J. Gómez-Gardeñes, M. Zanin, M. Romance, D. Papo, F. del Pozo, and S. Boccaletti, *Scientific Reports* **3**, 1344 (2013).
- [48] P. Kaluza, A. Kölzsch, M. T. Gastner, and B. Blasius, *Journal of the Royal Society: Interface* **7**, 1093 (2010).
- [49] M. Dickison, S. Havlin, and H. E. Stanley, *Physical Review E* **85**, 066109 (2012).
- [50] O. Yagan, D. Qian, J. Zhang, and D. Cochran, *IEEE JSAC Special Issue on Network Science* **31**, 1038 (2013).
- [51] C. Buono, L. G. Alvarez-Zuzek, L. A. Braunstein, and P. A. Macri, *PLOS ONE* **9**, e92200 (2014).
- [52] M. Tizzoni, P. Bajardi, C. Poletto, J. J. Ramasco, D. Balcan, B. Gonçalves, N. Perra, V. Colizza, and A. Vespignani, *BMC medicine* **10**, 165 (2012).
- [53] P.-S. Gsell, A. Camacho, A. J Kucharski, C. H Watson, A. Bagayoko, S. Danmadji Nadlaou, *et al.*, *The Lancet Infectious Diseases* **17**, 1276 (2017).
- [54] L. Valdez, R. H. Aragão, H. Stanley, and L. Braunstein, *Scientific reports* **5**, 12172 (2014).
- [55] M. F. C. Gomes, A. P. y Piontti, L. Rossi, D. Chao, I. Longini, M. E. Halloran, and A. Vespignani, *PLOS Current Outbreaks* (2014), doi:10.1371/currents.outbreaks.cd818f63d40e24aef769dda7df9e0da5.
- [56] C. Buono and L. A. Braunstein, *EPL (Europhysics Letters)* **109**, 26001 (2015).

- [57] L. G. Alvarez-Zuzek, H. E. Stanley, and L. A. Braunstein, *Scientific Reports* **5**, 12151 (2015).
- [58] L. G. Alvarez-Zuzek, C. Buono, and L. A. Braunstein, in *Journal of Physics Conference Series*, Vol. 640 (2015).
- [59] M. Molloy and B. Reed, *Random Structures and Algorithms* **6**, 161 (1995).
- [60] C. Lagorio, M. V. Migueles, L. A. Braunstein, E. López, and P. A. Macri, *Physica A* **388**, 755 (2009).
- [61] Y. Hu, S. Ji, L. Feng, S. Havlin, and Y. Jin, arXiv preprint arXiv:1509.03484 (2015).
- [62] P. Erdős and A. Rényi, *Publications Mathematicae* **6**, 290 (1959).
- [63] K. T. Alligood, T. D. Sauer, and J. A. Yorke, *CHAOS: An Introduction to Dynamical Systems* (Springer, 1997).
- [64] L. A. N. Amaral, A. Scala, M. Barthélemy, and H. E. Stanley, *Proc. Natl. Acad. Sci. USA* **97**, 11149 (2000).

## APPENDIX

### A. Dependence on $T_\beta$

In this section we show the dependence on the overall transmissibility  $T_\beta$  of the recovered and vaccinated fraction of nodes,  $R$  and  $V$ , in the steady state. Also, we show the dependence on the prefactors that multiply Eqs. (4) and (5), which measure the relative weight of the probabilities of infection (or vaccination) in the dynamic.

As we saw earlier in Sec. II B, from Eqs. (1) and (3) we find the prefactors in Eqs. (4) and (5) as,

$$\begin{aligned} B_\beta &= \frac{T_\beta}{T_\beta + T_\omega} = \frac{(1 - \omega) \beta}{(1 - \omega) \beta + \omega}, \\ B_\omega &= \frac{T_\omega}{T_\beta + T_\omega} = \frac{\omega}{(1 - \omega) \beta + \omega}. \end{aligned} \quad (8)$$

Note, interestingly these prefactors are independent of the recovery time  $t_r$ .

In Fig. 5 we plot in (a) the total fraction of recovered nodes  $R$ , (b)  $R/B_\beta$ , (c) total fraction of vaccinated nodes  $V$  and (d)  $V/B_\omega$ , as a function of the epidemic transmissibility  $T_\beta$  for different values of  $\omega$ , with  $\omega \in [0.1, 0.8]$  with  $\Delta\omega = 0.1$ . For the sake of simplicity we consider the case  $t_r = 1$ . Thus, from Eq. (1) the epidemic transmissibility is reduced to  $T_\beta = (1 - \omega)\beta$ .

The multiplex network consists of two coupled Erdős-Rényi (ER) networks with  $q = 0.3$ , average degree  $\langle k_A \rangle = \langle k_B \rangle = 5$  and,  $k_{min} = 0$  and  $k_{max} = 40$ .

As we can see, in Fig. 5(a) and (c) for the different  $\omega$  values, when  $R$  and  $V$  are plotted as a function of  $T_\beta$ , the dependence on  $\omega$  is lost. Thus, all the curves have the same critical threshold [56] and are equal to

$$T_\beta|_{(\beta=\beta_c)} = \frac{1}{\langle k \rangle (1 + q)}. \quad (9)$$

As we consider  $\langle k \rangle = \langle k_A \rangle = \langle k_B \rangle = 5$  and  $q = 0.3$ , then for Figure 5 the critical threshold is  $T_\beta|_{(\beta=\beta_c)} \simeq 0.15$ .

On the other hand, in Fig. 5(b) and 5(d) we multiply all the curves of the fraction of recovered in the y-axis by the weighted prefactor of infection and we can see that all data collapse into a single curve.

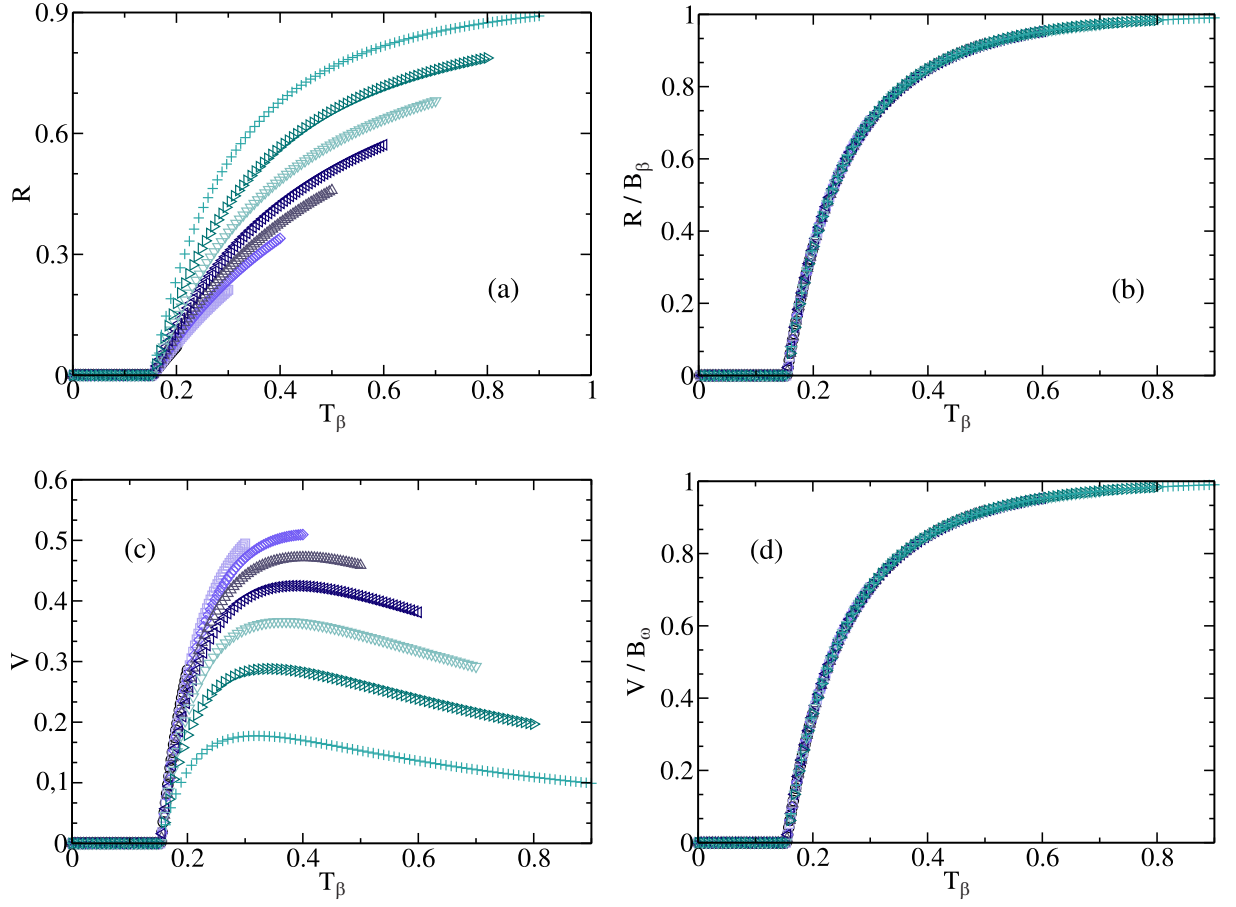


FIG. 5. **Theoretical Results** of the total fraction of (a) recovered  $R$ , (b)  $R/B_\beta$ , (c) vaccinated  $V$  and (d)  $V/B_\omega$  nodes as a function of the overall transmissibility  $T_\beta = (1 - \omega) \beta$  when  $t_r = 1$  and for different values of  $\omega$ , in the steady state. The multiplex network consists of two ER networks and we set  $q = 0.3$ . Each network size is  $N = 10^5$  and  $\langle k_A \rangle = \langle k_B \rangle = 5$  with  $k_{min} = 0$  and  $k_{max} = 40$ .